SAN099-2079J

COPPER WETTING of α-Al_2O_3(0001): THEORY AND EXPERIMENT

RECEIVED
AUG 18 1999
OSTI

J. A. Kelber*, Chengyu Niu, and K. Shepherd

Department of Chemistry, University of North Texas, Denton, TX 76203

D. R. Jennison and A. Bogicevic

Surface and Interface Sciences Department, Sandia National Laboratories,

Albuquerque, NM 87185-1421

ABSTRACT

XPS studies have been carried out on sputter deposited copper on a substantially hydroxylated α-Al_2O_3(0001) (sapphire) surface under ultra-high vacuum (UHV) conditions. XPS-derived Cu uptake curves show a sharp change in slope at a coverage of 0.35 monolayers (on a Cu/O atomic basis), indicative of initial layer-by-layer growth. Cu(LMM) lineshape data indicate that, prior to the first break in the curve, Cu is oxidized to Cu(I). At higher coverages, metallic Cu(0) is observed. These data agree with first principles theoretical calculations, indicating that the presence of ad-hydroxyl groups greatly enhances the binding of Cu to bulk sapphire surfaces, stabilizing Cu(I) adatoms over two-dimensional metallic islands. In the absence of hydroxylation, calculations indicate significantly weaker Cu binding to the bulk sapphire substrate and non-wetting. Calculations also predict that at Cu coverages above 1/3 monolayer (ML), Cu-Cu

DISCLAIMER

This report was prepared as an account of work sponsored by an agency of the United States Government. Neither the United States Government nor any agency thereof, nor any of their employees, make any warranty, express or implied, or assumes any legal liability or responsibility for the accuracy, completeness, or usefulness of any information, apparatus, product, or process disclosed, or represents that its use would not infringe privately owned rights. Reference herein to any specific commercial product, process, or service by trade name, trademark, manufacturer, or otherwise does not necessarily constitute or imply its endorsement, recommendation, or favoring by the United States Government or any agency thereof. The views and opinions of authors expressed herein do not necessarily state or reflect those of the United States Government or any agency thereof.

DISCLAIMER

Portions of this document may be illegible in electronic image products. Images are produced from the best available original document.

interactions predominate, leading to Cu(0) formation. These results are in excellent agreement with experiment. The ability of surface hydroxyl groups to enhance binding to alumina substrates suggests a reason for contradictory experimental results reported in the literature for Cu wetting of alumina.

I. INTRODUCTION

We report experimental and theoretical studies of Cu interactions with the sapphire basal plane, α-Al_2O_3 (0001), under ultra-high vacuum conditions. The interaction of metals with oxides is of basic scientific interest, and has been a subject of controversy[1,2]. Technological motivation includes the long-standing importance of such interactions in heterogeneous catalysis [3], high temperature metallurgy [4], and microelectronics, the latter recently assuming additional practical interest because of the introduction of Cu in modern integrated microcircuits [5]. Cu deposition onto diffusion/adhesion barriers or dielectrics under industrial conditions typically involves a partially oxidized metallic substrate. The ability to predict the relative strength of metal interactions with a "real world" oxide and understand growth morphology would have immediate impact on both processing and materials choices in microelectronics fabrication, and the areas of catalysis, adhesion, and corrosion inhibition. Here we combine experiment with first principles theory in an attempt to further such an ability.

Metal interactions specifically with alumina substrates present an important area for study because of the use of alumina in supported catalysts [3], and the experimental ability to produce ordered substrates in both thin film [4,6-10] and bulk-truncated forms. Experimental results [11-16] for Cu deposited onto alumina have been inconsistent. XPS studies [11] of Cu deposited by thermal evaporation onto bulk truncated α-Al_2O_3(0001) indicated ordered layer-by-layer growth for

the first 2-3 atomic layers. The initial Cu ad-layer was observed to form "Cu-O bonds" with the substrate [11] and was present as oxidized Cu, in the form of Cu(I) ions. Other studies on polycrystalline Al_2O_3 reported layer-by-layer growth [12,13] and Cu(I) formation at coverages below 0.5 monolayers [13]. In contrast, a study on epitaxial ~ 20 Å Al_2O_3 films formed on refractory metal substrates [14] reported the growth of 3-dimensional clusters of metallic Cu, even at submonolayer Cu coverages. In particular, XPS and low energy ion scattering (LEIS) measurements [14] indicated Cu cluster formation at the lowest observable coverages at both 300 K and 80 K, with no Cu(I) observed. XANES [15] measurements carried out on sapphire substrates have reported no evidence of Cu oxidation, and coverage-dependent shifts in Cu core level and LMM peaks have been interpreted in terms of final state screening [16], rather than ionization of the Cu. Meanwhile, recent ion scattering experiments by Ahn and Rabalais [17] have shown that cut and polished sapphire(0001) surfaces (the basal plane is not a cleavage surface) cannot be made free of hydrogen contamination in the form of hydroxyl even by annealing to 1400K. In addition, experimental studies of Rh deposited on ultrathin epitaxial Al_2O_3 films [18] suggest that surface hydroxyl binds the Rh to the surface as a cation and serve as nucleation sites for Rh clusters. These studies have raised the issue of the role of surface hydroxyl groups in producing the apparent disagreements summarized above. The experimental results reported below indicate initial layer by layer growth of Cu on hydroxylated α-Al_2O_3(0001) at 300K, and the exclusive presence of Cu(I) during the formation of the first layer. Analysis of x-ray excited Cu(LMM) Auger data indicate that changes in the spectra are due to changes in the initial electronic state of the copper rather than to final state screening effects.

A few ab-initio studies of Cu on Al_2O_3 have been reported [19]. These early studies indicate a very weak interaction between Cu adatoms and the substrate. Such findings are in

marked contrast to the theoretical results reported here, because relaxation of the oxide surface, not possible in small cluster models [19], has been found to critically determine the nature of adsorption [20,21]. Another important difference between the methods used here and in previous studies [19] is the employment of thick slabs, made possible by advances in computing and algorithms [20]. The surface relaxation in sapphire(0001) is unusually large and deep, and necessitates slabs thicker than about 8 oxygen layers for quantitative reliability.

The first accurate theoretical study of metals on sapphire [20] found two very different adsorption mechanisms, depending on coverage. While isolated adatoms are oxidized and bind strongly as ions, if coordinated to two or more other metal adatoms, the adsorbates are metallic, showing negligible charge transfer to the surface and relatively weak adsorption, mainly by polarization. With a few interesting exceptions not relevant to the present paper, this basic pattern of binding was also found when 11 different metals were studied adsorbed on an ultrathin (~5 Å) Al_2O_3 film [21]. In the latter study, Cu was noted to differ qualitatively from metals such as Pd and Pt, in that the strength of the bonding as an oxidized species is stronger due to the smaller ionic radius, while the strength of the metallic Cu-Cu interactions is weaker due to reduced cohesive energy.

Born-Haber cycles can be computed to predict thermodynamically whether a deposited metal would rather spread out on the surface as isolated adatoms or be drawn into 2D islands [20,21]; one can also, of course, compare 2D islands with 3D islands. It is then possible, if the oxidized isolated adatoms are sufficiently bound compared with the metallic atoms in 2D islands, for wetting to occur, even if 3D islands are preferred energetically over the others. In this case, 2D islands would act as kinetic barriers to 3D island formation from isolated adatoms(ions); however, if isolated adatoms are sufficiently mobile, the presence of defect nucleation sites for 3D clusters

(vide infra) could then deplete the numbers of isolated adatoms by direct adsorption and thus prevent the observation of a wetted surface. These issues will be discussed below in light of the experimental data.

Recently, defect nucleation sites for Pt clusters on MgO(100) have been studied using first principles calculations [22]. The two most common isolated surface defects were investigated: vacancies, both isolated and paired, and water byproducts, as both ad-OH and in-surface OH, the latter produced by the reaction of H^+ with a surface O^{2-} ion. It was found that single surface vacancies in fact destabilize Pt dimers (the first step in nucleation), while in contrast mixed divacancies and ad-OH impurities stabilize same, promoting metal island formation. In addition, it was found that ad-OH increases the adatom binding energy significantly. These results are likely to be quite general for highly ionic oxides, including sapphire. In fact, the above mentioned experimental studies of Rh deposition on hydroxylated ultrathin alumina films[18] clearly show an increase in the density of nucleation sites. Here, however, the surface is much more hydroxylated and the consequences quite different.

We report below on the binding and growth of Cu on α-Al_2O_3(0001) with a likely presence of 1/3-1/2 ML of hydroxyl impurities. Section II presents descriptions of the experimental and theoretical methods used in this study. Section III presents experimental results, while Section IV contains a description of theoretical results. Discussion is presented in Section V, and a summary and conclusions are contained in Section VI.

II. METHODOLOGIES

A. Experimental Methods

Experiments were carried out in a combined UHV analysis/sputter deposition system at the University of North Texas. The analysis and sputter deposition chambers were independently pumped by turbomolecular pumps to tolerate high gas loadings. Chamber isolation is achieved with differentially pumped Teflon seals against the polished double-walled manipulator rod. This arrangement permits sample transport on the rod between the analysis and sputter deposition environments. The sample, 10 x 10 x 0.5 (mm) of commercially obtained α-Al_2O_3(0001), was mounted on a Tantalum sample holder attached to two Tantalum leads which were themselves in contact with a liquid nitrogen reservoir. A combination of liquid nitrogen cooling and resistive heating of the sample holder permits a variation in temperature between 130 K and ~1100 K. All results reported here, however, were obtained at ambient temperature, ~300 K.

The sample was cleaned by sonication in acetone, methanol and deionized water prior to insertion in the vacuum system. Working pressures in the analysis chamber were in the range of 1-5 x 10^{-9} Torr, and in the range of 10^{-8}--10^{-7} Torr in the sputter deposition chamber (in the absence of plasma). Pressures in both chambers (in the absence of plasma) were monitored by nude ion gauges in both chambers placed out of line of sight of the sample. Pressures during plasma-induced sputter deposition were monitored with a baratron gauge.

XPS spectra were acquired using a commercially available hemispherical sector analyzer (VG100AX) operated at a constant pass energy of 50 eV. Calibration of the analyzer energy scale was carried out using sputter-cleaned Cu and Au samples, according to established techniques [23]. Mg Kα radiation was obtained from a commercial, unmonochromatized source (Physical

Electronics, PHI Model 1427) operated at 15 kV and 300 W. Software for data acquisition and analysis have been described previously [24]. Elemental atomic sensitivity factors appropriate to this analyzer (obtained from VG Microtech, UK) were used to estimate surface coverages and chemical composition from the integrated intensities of core-level transitions. XPS spectra were acquired with the sample aligned normal to the analyzer axis (normal incidence) and at 60°(with respect to the surface normal -grazing incidence).

The sputter gun (Physical Electronics) was operated by direct Ar gas feed into the ionization chamber with a variable excitation voltage of 1-5 KeV. Sputter deposition of Cu was carried out using a commercial water-cooled magnetron source (MiniMak), and an Ar plasma with a partial pressure of 0.015 Torr. Plasma power was readily maintained so as to give highly reproducible deposition rates as low as 0.01 ML Cu/min. This mechanism resulted in the deposition of Cu free from oxygen contamination, as determined by XPS measurements of films deposited on oxygen-free substrates (e.g., polyethylene). Cu depositions were carried out with the sample temperature initially at 300 K. Negligible increases in sample temperature were observed during plasma deposition. Repeated exposure of the sample to the environment of the sputter deposition chamber resulted in an unavoidable accumulation of adventitious carbon of the sample. Carbon coverage, however, appeared to saturate at ~0.5 monolayers (on a carbon to oxygen atomic basis), and was usually significantly lower (~0.1- 0.3 monolayers). Some trace contamination due to Ca impurities in the sapphire was also observed. No carbon contamination was observed as a function of Cu deposition. Deliberate variation of carbon coverage between 0.1 and 0.5 monolayers (e.g., by varying sample exposures to the vacuum of the deposition chamber prior to deposition) had no significant effect on Cu nucleation behavior or oxidation state.

B. Theoretical Methods

The electronic structure calculations were performed using the Vienna Ab Initio Simulation Package (VASP) [25]. This plane-wave based density-functional [26] code uses the ultrasoft pseudopotentials of Vanderbilt [27] which permit good convergence at a plane wave cutoff of 270 eV. For "standard" local density theory, we used the Perdew/Zunger parameterization [28] of the Ceperley/Alder electron gas results [29]. Geometric relaxation, to forces < 0.05 eV/Å, was done through a quasi-Newton algorithm. A damped dynamics method was found to speed the final relaxation process. The vacuum between repeating slabs exceeded 18 Å. Our slabs had nine layers of three O and two Al atoms per unit cell, with Cu and/or OH added to both sides. The center three Al_2O_3 layers were frozen at the bulk LDA spacing, while all other atoms were geometrically free to relax. We considered the most favored sites, which for 1/3 ML Cu is the hollow site above the deepest Al ion (Fig. 1) [19,20], and for 1 ML Cu is atop O [20]. We also considered 1/3 ML of ad-OH placed above the shallowest Al ion (the obvious site based on electrostatics), with and without 1/3 ML and separately 1 ML of Cu in sites O, which maximize the interaction with the OH. (The relaxed adsorbate positions with ad-OH present are distortions of these beginning positions.)

III. EXPERIMENTAL RESULTS

A. Vicinal and Lightly Sputtered Sapphire Surfaces

After insertion into the UHV chamber, XPS survey and core level spectra were obtained for the sapphire surface before annealing, after annealing to 1100 K in 5 x 10^{-6} Torr O_2, and after subsequent light Ar ion sputtering (1 KeV, 6 min) and annealing to 1100 K in O_2 (P=5.0 x 10^{-6} Torr) or UHV for 1 hour. Observed O(1s), Al(2p) stoichiometries derived from core-level

intensities are shown in Table I. Relative O and Al atomic concentrations in the XPS analysis region can be derived from XPS intensities[30]according to:

$$(1) \qquad N_O/N_{Al} = (I_O' \times S_{Al})/(I_{Al}' \times S_O)$$

Where N, S and I' are, respectively, the atomic concentrations, atomic sensitivity factors and XPS signal intensity from the very top monolayer. I' can be derived using

$$(2) \qquad I' = \int_{x=0}^{1} e^{-x/\lambda} dx \Big/ \int_{x=0}^{\infty} e^{-x/\lambda} dx$$

where λ is the mean free path length for O(1s) or Al(2p) potoelectrons in units of monolayers—5.2 monolayers and 7.2 monolayers, respectively[30].

As shown in Table I, the light sputtering treatment (which reduces contaminant carbon below observable levels) does not result in significant change in relative O and Al core level XPS intensities. O(1s) and Al(2p) spectra obtained after sputtering are displayed in Figs. 2 and 3 respectively. Binding energies and peak shapes were unchanged from those observed prior to the final sputter/anneal treatment.

Core level binding energies, as observed and compared with corresponding literature values, are summarized in Table II. Deviations in the observed binding energies from the corresponding literature values indicate that the amount of charging increases with binding energy (decreased kinetic energy), as expected if charging is a function of the inelastic mean free path of the photoelectrons. Comparison of normal incidence vs. grazing incidence results shows that differential charging is more pronounced with greater sampling depth. Such differential charging has been reported previously [11, 31-34] in studies on insulating substrates. Correction for such

differential charging effects is obviously more problematic than for uniform charging. The core level spectra listed in Table II were assigned to the literature values given. This makes it difficult, however, to precisely correct for shifts in the Cu(2p) and Cu(LMM) spectra in order to obtain accurate Cu Auger parameters (Auger Parameter = BE(Cu 2p3/2) + KE(Cu(LMM)). Therefore, characterization of the deposited copper by values of Cu Auger parameters must be regarded with considerable suspicion in these experiments. For this reason, we rely on well known changes in the Cu(LMM) lineshape [35,36] to characterize the electronic state of Cu ad-atoms, and avoid making any judgements based on the value of the Cu Auger parameter. The Cu(LMM) lineshape was determined to be independent of sample charging, which could be varied by changing the x-ray source-to-sample distance.

The O(1s) spectra obtained after light sputtering (Fig. 2), at grazing and normal incidence, are both well fit by two components (each with FWHM = 2.4 eV) with a minor peak at 1.3 eV higher binding energy than the major peak. Also in agreement with previous reports [11], the relative intensity of the higher binding energy component compared to the main peak is increased in the grazing incidence spectrum, indicating that this component corresponds to a surface species and is assigned to surface hydroxyl groups. The presence of hydrogen in the sapphire surface region, even after extensive annealing in UHV, has been confirmed by ion-scattering experiments [17]. The Al(2p) spectra are well fit by a single spectral component. The relative O and Al concentrations derived from normal incidence measurements (Table I) are as expected for stoichiometric sapphire, for both the initial and 1 KeV sputtered surfaces. Ratios obtained from grazing incidence spectra, however, indicate oxygen enrichment (Table I). These data are again consistent with hydroxylation of the surface.

An estimate of the surface hydroxyl coverage can be as follows[30]:

(3) $I_B = I_B^{\infty}\{1-\Phi_A+\Phi_A\exp[-a_A/\lambda_A(EB)\cos\theta]\}$

I_B is the O(1s) signal intensity from the substrate(covered by –OH), I_B^{∞} is the O(1s) signal from a pure substrate, a_A is the diameter of –OH(~2.8Å[37]), λ_A is the mean free path for O(1s) electrons(~11Å[30,38]), and θ is the angle between the analyzer lens axis and the surface normal. Using the total O(1s) peak area as I_B^{∞}, an initial –OH surface coverage of 0.47 ML is obtained. This coverage is not affected by either annealing to 1100 K in UHV or O_2, consistent with previously reported results[17].

B. Cu Deposition

Results of Cu deposition were the same on unsputtered and lightly sputtered surfaces, and are shown below for the latter (which is carbon free before deposition). Fig. 4a shows x-ray excited Cu(LMM) spectra as a function of Cu deposition time. The evolution of the Auger lineshape indicates that for deposition times < 12 minutes, Cu is present as Cu(I). At longer deposition times (higher coverages), the evolution of a new feature at approximately 3 eV higher kinetic energy (corresponding to a higher Auger parameter) indicates the onset of Cu(0) formation [35,36]. In order to determine that the Cu(I) formation observed at low coverages was not an artifact of contamination from the chamber ambient, or in some way due to the use of sputter deposition instead of thermal evaporation, a similar experiment was carried out for Cu deposition on a ~ 1000 Å film of amorphous SiO_2 grown on a Si wafer substrate. Cu is well known to interact only weakly with SiO_2 surfaces[39]. The results for Cu/SiO_2 (Fig. 4b) indicate the presence of

Cu(0) even at the lowest observable coverages. Therefore the presence of Cu(I) on sapphire at low coverages is due to Cu ad-atom interaction with the substrate, and not due to experimental artifacts.

The change in relative Cu(2p3/2) XPS intensity (normalized to the O(1s) intensity) with Cu deposition (the uptake curve) is shown in Fig. 5 for Cu on sapphire. The uptake curve on sapphire (Fig. 5) shows a sharp change in slope, which is indicative of layer-by-layer growth (wetting)[30]. A comparison of Figs. 4a and 5 indicates that the appearance of Cu(0) corresponds to the completion of the first layer; i.e., the first layer consists of Cu(I). The Cu coverage at which this change in slope occurs can be calculated from XPS intensities according to equation (2). Estimating mean free path values from the universal curve [38] yields a value of 9 Å for the Cu(2p3/2) transition, and 11 Å for the O(1s) transition. These data therefore indicate that the initial Cu(I) ad-layer grows to a maximum coverage of ~0.35 monolayer (on a Cu/O atomic basis), at which point formation of Cu(0) occurs on top of the Cu(I) ad-layer.

C. Thermal Stability of the Cu-Adlayers

The thermal stability of the deposited Cu was tested by annealing the Cu-modified surface to temperatures up to 1000 K in UHV. The annealing behavior of Cu strongly depends on total Cu coverage. As shown in Figs. 6 and 7, a 0.25 ML coverage of Cu (pure Cu(I)) is stable up to 1000 K without significant change in either relative Cu (2p3/2) intensity or change in oxidation state (Fig. 7a). At 0.75 ML coverage, however, both Cu(I) and Cu(0) are present. Annealing to elevated temperatures now results in a notable reduction in the total relative Cu intensity (Fig. 6). Coincident with this, the portion of the Cu(LMM) spectrum corresponding to Cu(I) shows a marked decrease in relative intensity compared to the Cu(0) component. (An examination of the

Cu(2p) spectrum reveals that no observable amounts of Cu(II) are present at any time during this procedure.)

The data in Figs. 6 and 7a indicate that, at 0.75 ML, annealing to slightly elevated temperatures (~500 K or higher) results in the formation of 3-D nuclei of metallic Cu, including the Cu(I) originally present at the surface. At such low temperatures, desorption of Cu from the surface can be discounted. If only the Cu(0) originally present at 300 K were involved in the nucleation (de-wetting) process, then one would expect an increase in the relative Cu(I) intensity in the Cu(LMM) spectrum. Therefore, the data in Figs. 6 and 7 indicate that the presence of Cu(0) causes Cu(I) to de-wet from the surface at relatively low temperatures. In the absence of Cu(0), Cu(I) is stable on the surface to at least 1000 K.

IV. Theoretical Results

In Table III, we present the LDA adsorption energy of Cu at 1/3 and 1 ML coverage at the strongest binding sites [20] on the sapphire surface. We find that when isolated, Cu adatoms are oxidized and bind strongly. We also show the results of a Born-Haber analysis, where the tendency to form 2D islands is given by a negative value (no wetting) of $\Delta E = E(1ML\ Cu) + 2E(clean\ surface) - 3E(1/3\ ML\ Cu)$. Cu adatom binding is sufficiently weak on clean sapphire surface so 2D islanding is favored over wetting.

In Table III, we also see similar results for the hydroxylated surface. Here, Cu adatom binding is more than doubled, as is also the binding at 1 ML. Now we see that the substantial number of OH groups has reversed the Born-Haber prediction of the clean surface, and wetting is indeed preferred, as observed.

Finally, we also examine a possible reaction of Cu at 1 ML with OH, leading to OH dissociation. We find this is exothermic by 0.6 eV per unit cell. In the relaxed geometry in this

case, the H is associated with metallic Cu far from the adoxygen left behind, while the latter is closely coordinated to two Cu atoms. However, this result does not alter the wetting prediction (Table III).

V. DISCUSSION

The experimental results presented above demonstrate that Cu will wet a substantially hydroxylated α-Al_2O_3(0001) surface at 300 K. The initially deposited Cu forms a conformal Cu(I) ad-layer with a maximum coverage of ~0.35 ML (on a Cu/O basis). At higher coverages, Cu(0) forms over the initial Cu(I) ad-layer. These results are in excellent agreement with theoretical calculations performed on thick slabs, which show that hydroxylation should significantly increase the binding of Cu to the sapphire (0001) surface, and that maximum Cu(I) coverage will be limited by the fact that at higher coverages, Cu-Cu interactions causing metallic Cu would predominate. In fact, the reaction of the additional Cu(0) with the initial Cu(I) is observed to be activated by an increase in temperature.

The experimental and theoretical results strongly suggest a rationale for the wide range of contradictory results [11-16] reported for Cu wetting of alumina surfaces. First, the degree of sapphire surface hydroxylation is not obvious from a routine inspection of the XPS data of the clean surface, and a reading of the relevant reports [11-17] indicates that surface hydroxylation was not a prominent concern for many experimental groups. Second, thin alumina films are much more readily de-hydroxylated by being produced and by annealing in UHV than are sapphire surfaces [17,40]. Therefore, in comparing literature results, one is most likely comparing substantially hydroxylated sapphire surfaces to unhydroxlyated or lightly hydroxylated thin films

(polycrystalline or epitaxial). The theoretical and experimental results shown here predict that Cu growth on alumina should vary greatly with the degree of surface hydroxylation. In this regard, it is useful to note results recently reported for Cu deposited on presumably dehydroxylated epitaxial Al_2O_3 films ~ 20 Å thick [14], which clearly indicate that Cu does not wet the surface. In summary, the Cu/alumina binding is predicted to be significantly affected by both surface hydroxylation and alumina substrate thickness.

The experimental results (Figs. 6 and 7) also show that the thermal stability of adsorbed Cu(I) species is decreased in the presence of Cu(0). The thermal stability of very low coverages of Cu on sapphire (hydroxyl coverage undetermined) has been previously characterized by Auger spectroscopy[41]. Those results indicated that at very low coverages, the Cu ad-layer was stable to at least 700 K[41]. Those results are in agreement with those presented here, which indicate that the initial layer (Cu(I)) is stable on the hydroxylated basal plane of sapphire to ~1000 K. Subsequently deposited Cu(0), however, will not only nucleate (de-wet) at relatively low temperatures, but will also cause the apparently tightly bound Cu(I) to de-wet from the surface. Such behavior is quite different from what is observed, for example, in the Cu/W(100) system[42], where the first Cu adlayer is tightly bound to the substrate whether or not a subsequent layer is present. The temperatures at which decreases in Cu(I) coverage are observed (~ 500 K, fig. 6) are sufficiently low as to rule out dehydroxylation of the surface as a cause of this behavior.

We have not computed the hopping energy for Cu(I) on a sapphire surface, but activation energies of 0.4-0.5 eV have been reported for Pt adatoms on (non-hydroxylated) Al_2O_3/NiAl(110)[43], and computed Pt binding energies for this surface are ~ 3 eV by LDA [20]. Here, however, one CANNOT assume the same ratio between hopping barrier and binding energy,

because while hopping on the clean surface might involve an activation barrier similar to the hollow-to-atop energy difference (< 1 eV), hopping on hydroxylated sapphire would involve hopping from the adjacent site to an ad-OH (binding energy ~5.2 eV) to a site away from the ad-OH (clean surface binding energy ~1.8 eV), resulting in an activation energy of > 3 eV. Assuming a reasonable prefactor of $\sim 10^{12}$, this implies rapid diffusion (on experimental time scales) on the clean surface but negligible diffusion on the hydroxylated surface. In addition to slow diffusion, dimerization in the absence of Cu(0) is obviously hindered by Cu(I)-Cu(I) repulsion. These arguments could explain the high temperature stability of Cu(I) at lower coverages. At higher coverages, the presence of Cu(0) would facilitate dimerization and metal island nucleation, the latter of which would irreversibly reduce the Cu(I), as observed.

We have no information concerning the detailed morphology of the prepared surface, such as the density of steps, point defects, etc. The fact that wetting has been observed on both ordered bulk (sapphire) [11] and disordered (polycrystalline film) surfaces [12], while non-wetting as also been reported for bulk sapphire[15,16] and for epitaxial films[14], indicates that the transition from wetting to non-wetting does not depend on such details of surface topography. In addition, the experimental results reported here are observed to be independent of adventitious carbon, at least up to coverages of ~ 0.5 ML. This indicates that such contamination does not critically impact wetting behavior under these conditions and therefore the results presented here are of relevance to situations of practical industrial processing.

In view of the above results demonstrating enhanced binding of Cu, as Cu(I), to hydroxylated sapphire surfaces, the mechanical adhesion results for Cu overlayers deposited on unsputtered and pre-sputtered sapphire surfaces are of interest[44]. Those studies observed an order of magnitude increase in Cu/sapphire mechanical adhesion for an optimum amount of Ar+

sputtering of the sapphire surface prior to Cu deposition, followed by annealing of the interface after deposition. The authors concluded that pre-sputtering might induce an interfacial alloy which would lead to enhanced adhesion, as suggested by Cu Auger and photoemission spectra. We must therefore conclude that the effects of hydroxylation explored here are only one aspect of interfacial wetting/adhesion, and that defects (vacancies, dehydroxylation, etc.) induced by sputtering of sapphire or perhaps other alumina surfaces may trigger new interfacial reaction pathways at elevated temperatures.

VI. CONCLUSIONS

Experimental studies have examined the deposition of Cu on a substantially hydroxylated α-Al_2O_3(0001) (sapphire) substrate at 300 K under UHV conditions. The results agree with a conceptual model from first principles theoretical calculations on Cu adsorption on hydroxylated sapphire. The results include the following:

(1) Cu deposition onto hydroxylated sapphire(0001) at 300 K results in initial Cu wetting of the substrate and layer-by-layer growth.

(2) The initial Cu adlayer is oxidized to Cu(I), with a maximum surface coverage of ~0.35 monolayers on a Cu/O atom basis. This is in good agreement with theoretical calculations which predict a maximum coverage of Cu(I) of 0.33 monolayers, due to the predominance of Cu-Cu interactions at higher coverages.

(3) In the absence of Cu(0), adsorbed Cu(I) is stable on the hydroxylated sapphire surface up to at least 1000 K. In the presence of Cu(0), Cu(I) is destabilized at ~ 500 K or greater, and begins to join in the formation of 3-D Cu(0) nuclei.

Acknowledgements:

The authors acknowledge useful discussions with Ted Madey and with H.-J. Freund. VASP was developed at the Institut fur Theoretische Physik of the Technische Universitat Wien. Work at UNT was supported in part by the U.S. Department of Energy, Office of Basic Energy Sciences, under grant no. DE-FG03-93ER45497, and in part by the Robert Welch Foundation, under grant no. B-1356, which are gratefully acknowledged. Sandia is a multiprogram laboratory operated by Sandia Corporation, a Lockheed-Martin Company, under Contract DE-AC04-94AL85000. This work was partially supported by a Sandia Laboratory Directed Research and Development Project.

REFERENCES

1. R. J. Lad, *Surface Review and Lett.* **2**, 109 (1995)

2. V. E. Heinrich and P. A. Cox, *The Surface Science of Metal Oxides* (Cambridge University Press, Cambridge 1994) pp. 378-458

3. G. Ertl and H.-J. Freund, *Physics Today* (January, 1999) 32

4. F. H. Stott, *Rep. Prog. Phys.* **50**, 861 (1987)

5. *National Technology Roadmap for Semiconductors*, Semiconductor Industry Association (San Jose, CA 1997)

6. Ming-Cheng Wu and D. Wayne Goodman, *J. Phys. Chem.* **98**, 9874 (1994)

7. Yutong Wu, E. Garfunkel and T. E. Madey, *J. Vac. Science and Technol.* **A14**, 2554 (1996)

8. R. M. Jaeger, H, Kuhlenbeck, H.-J. Freund, M. Wuttig, W. Hoffman, R. Franchy and H. Ibach, *Surf. Sci.* **259**, 235 (1991)

9. G. F. Cotterill, H. Niehus and D. J. O'Connor, *Surf. Rev. and Lett.* **3**, 1355 (1966)

10. C. Becker, J. Kandler, H. Raaf, R. Linke, T. Pelster, M. Drager, M. Tanemura and K. Wandelt, *J. Vac. Science and Technol.* **A16**, 1000 (1998)

11. S. Varma, G. S. Chottiner, and M. Arbab, *J. Vac. Science and Technol.* **A10**, 2857 (1992)

12. J. G. Chen, M. L. Colaianni, W. H. Weinberg and J. T. Yates, Jr., *Surf. Sci.* **279**, 223 (1992)

13. F. S. Ohuchi, R. H. French and R. V. Kasowski, *J. Appl. Phys.* **62**, 2286 (1987)

14. Y. Wu, E. Garfunkel and T. E. Madey, Jr. *J. Vacuum Science and Technology* **A14**, 1662 (1996)

15. S. Gota, M. Gautier, L. Douillard, N. Thromat, J. P. Duraud and P. LeFevre, *Surf. Sci.* **323**, 163 (1995); see also M. Gautier, L. Pham Van and J. P. Duraud, *Europhys. Lett.* **18**, 175 (1992)

16. V. Vijayakrishnan and C. N. R. Rao, *Surf. Sci. Lett.* **255**, L516 (1991)

17. J. Ahn and J. W. Rabalais, *Surf. Sci.* **388**, 121 (1997)

18. J. Libuda, M. Frank, A. Sandell, S. Andersson, P. A. Bruhwiler, M. Baumer, N. Martensson and H.-J. Freund, *Surf. Sci.* **384**, 106 (1997)

19. V. D. Castro, G. Polzonetti and R. Zanoni, *Surf. Sci.* **162**, 348 (1985); see also K. H. Johnson and S. V. Pepper, *J. Appl. Phys.* **83**, 6634 (1982)

20. C. Verdozzi, D. R. Jennison, P. A. Schultz and M. P. Sears, **82**, 799 (1999)

21. A. Bogicevic and D. R. Jennison, *Phys. Rev. Lett.* **82**, 4050 (1999)

22. A. Bogicevic and D. R. Jennison (~~submitted~~)

23. C. J. Powell, *Surf. and Interface Analysis* **23**, 121 (1995)

24. D. Martini, K. Shepherd, R. Sutcliffe and J. Kelber, and H. Edwards and R. San Martin, *Appl. Surf. Sci.* **141**, 89 (1999)

25. G. Kresse and J. Hafner, *Phys. Rev. B,* **47**, 558 (1993); **49**, 14251 (1994); **54**, 11169 (1996)

26. P. Hohenberg and W. Kohn, *Phys. Rev.* **136**, B864 (1964); W. Kohn and L. J. Sham, Phys. Rev. **140**, A1133 (1964)

27. D. Vanderbilt, *Phys. Rev. B,* **41**, 7892 (1990)

28. J. Perdew and A. Zunger, *Phys. Rev. B* **23**, 5048 (1981)

29. D. M. Ceperley and B. J. Alder, *Phys. Rev. Lett.* **45**, 566 (1980)

30. M. P. Seah, in *Practical Surface Analysis (2nd Edition) Vol. 1: Auger and Photoelectron Spectroscopy*, D. Briggs and M. P. Seah (editors), (J. Wiley and Sons, Ltd., Chichester, UK: 1983) pp. 201-255)

31. T. L. Barr, *J. Vac. Science and Technol.* **A7**, 1677 (1989)

32. Xiang-rong Yu and H. Hantsche, *Surface and Interface Analysis,* **20,** 555 (1993)

33. A. J. Pertsin and Yu. M. Pashunin, *Appl. Surface Science* **44**, 171-78 (1990)

34. J. Cazaux and P. Lehuede, *J. Electron. Spec. and Rel. Phenom.* **59**, 49 (1992)

35. A. J. Pijpers, K. Berreshelm and M. Wilmers, *Fresenius J. Anal. Chem.* **346**, 104 (1993)

36. T. H. Fleisch and G. J. Mains, *Applications of Surface Science* **10**, 51 (1982)

37. *CRC Handbook of Chemistry and Physics (74th Edition)*, D. R. Lide and H. P. R. Frederikse (editors) (CRC Press, Ann Arbor, MI; 1993) p.12-8

38. G. A. Somorjai, *Introduction to Surface Chemistry and Catalysis* (J. Wiley and Sons, NY; 1993) p. 383

39. J. B. Zhou, T. Gustafsson and E. Garfunkel, *Surf. Sci.* **372**, 21 (1997)

40. B. G. Frederick, G. Apai and T. N. Rhodin, *Surf. Sci.* **277**, 337 (1992)

41. Qinlin Guo and Preben Møller, *Surface Science* **244**, 228 (1991)

42. E. Bauer, H. Poppa, G. Todd and F. Bonczek, *J. Appl. Phys.* **45**, 5164 (1974)

43. N. Ernst, B. Duncomb, G. Bozdech, M. Naschitzki, and H.-J. Freund, et al., *Ultramicroscopy (in press)*

44. J. E. E. Baglin, *Nucl. Inst. and Methods in Phys. Res.* **B39**. 764 (1989)

Table I. Sapphire(0001) Surface O to Al atomic ratio* after Ar^+ sputtering at 1, 2, and 5 KeV for 10 minutes.

θ**	Initial	1 KeV	2 KeV	5 KeV
0°	1.54	1.52	1.51	1.49
60°	1.73	1.72	1.61	1.45

* Relative standard deviation: 3%.
** θ is the angle between the analyzer lens and the sample surface normal.

Table II. Initial Sapphire sample Core level binding energies (eV) and differential charging (indicated within parentheses).

XPS line	Al(2p)	C(1s)	O(1s)
Literature values	74.4	284.5	531.0
Normal incidenc	88.91 (14.5)	298.40 (13.9)	543.74 (12.7)
Grazing incidenc	87.82 (13.4)	297.60 (13.1)	543.24 (12.2)

* From *Handbook of X-Ray Photoelectron Spectroscopy* (1995) by Physical Electronics, Inc.

Table III. The LDA adsorption energy of Cu on a per atom basis in eV on clean sapphire(0001), ~~on and ultrathin film of Al_2O_3 (from Ref. [22])~~, and on hydroxylated sapphire with 1/3 ML of ad-OH. The Born-Haber energy ΔE_{01} is positive when wetting occurs.

Cu coverage	1/3 ML	1 ML	ΔE_{01}
Sapphire	1.8	0.5	-4.5
~~5 Å film~~	~~4.6~~	~~0.9~~	~~+3.5~~
Sapphire+OH	5.2	1.1	+3.8
Above with dissociated OH	--	1.3	+3.1

Figure Caption

Figure 1. Representation of the sapphire(0001) surface showing the most favored sites for ("a") 1/3 ML Cu (hollow sites above the deepest Al cations) and ("b") 1 ML Cu (atop O). (See reference 19 and 20 ~~for detail~~.

Figure 2. O(1s) spectra(without charging correction) of sapphire(0001): (a) normal incidence; (b) 60° grazing incidence. Both are well fit by two components: a major O^{2-} peak and a minor OH peak at 1.3 eV higher binding energy (FWHM 2.4 eV).

Figure 3. Al(2p) spectra(without charging correction) of sapphire(0001): (a) normal incidence; (b) 60° grazing incidence. Both are well fit by a single component with FWHM of 2.2 eV.

Figure 4. Cu(LMM) evolution during Cu deposition on (a) sapphire(0001) and (b) SiO2 with deposition rate at 0.03 ML Cu/minute. Deposition temperature = 300K.

Figure 5. Cu(2p)/O(1s) ratio vs. deposition time for Cu on sapphire(0001) (deposition rate at 0.03ML Cu/min). Cu(I) grows to a maximum coverage of ~0.35ML, after which Cu(0) formation was observed. The sharp change in slope indicates a layer by layer growth mode.

Figure 6. Cu(2p)/O(1s) ratio during annealing of 0.25 and 0.75 ML Cu deposited on sapphire(0001). Dewetting of Cu occurred at 500-600K for coverage of 0.75 ML. No dewetting was observed up to 1000K for 0.25 ML coverage.

Figure 7. Cu(LMM) line shape change during annealing of (a) 0.75 ML (b) 0.25 ML Cu deposited on sapphire(0001) (kept 20 minutes at each temperature). While Cu(I) stable up to 1000K at low coverage(0.25 ML), Cu(I) reduction to Cu(0) was observed as early as 500K at high coverage(0.75 ML).

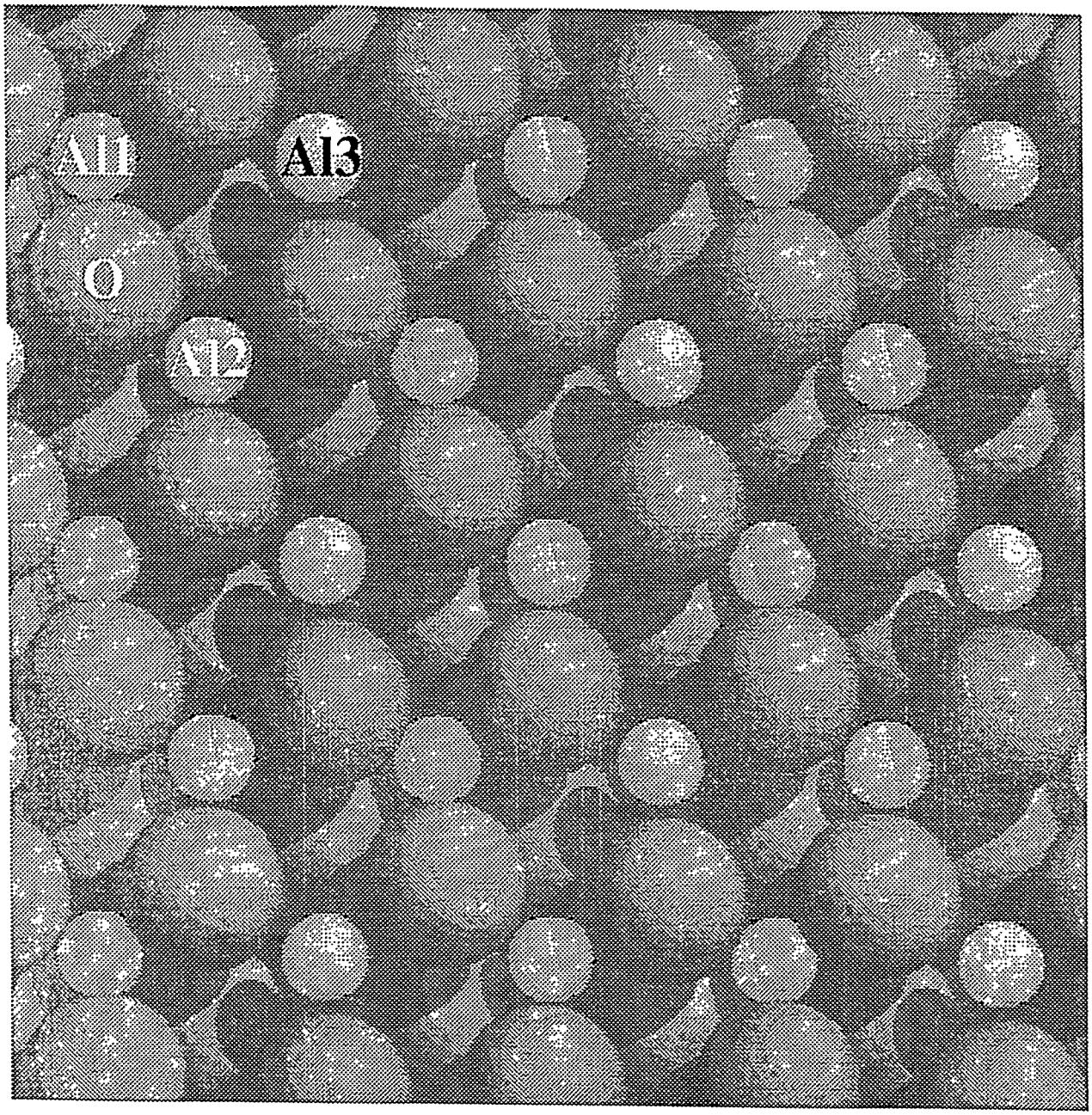

Figure 1.

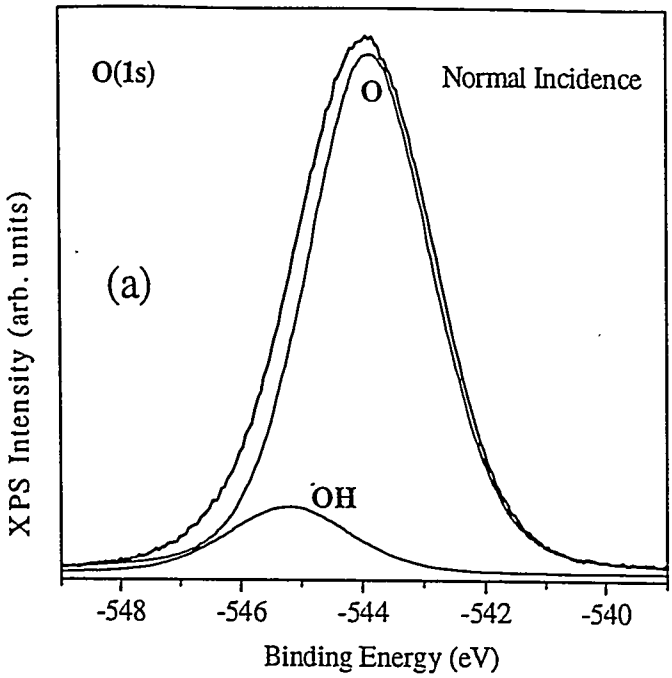
O(1s)
Normal Incidence
O
(a)
OH
XPS Intensity (arb. units)
-548
-546
-544
-542
-540
Binding Energy (eV)

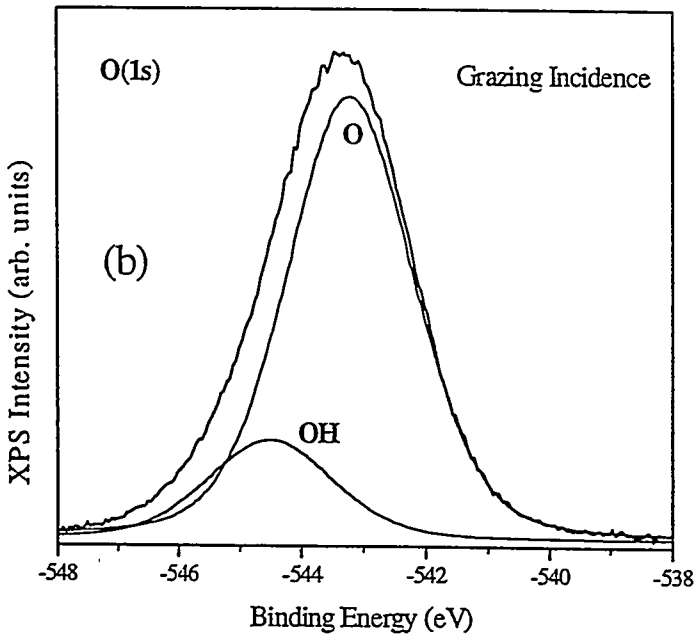
O(1s)
Grazing Incidence
O
(b)
OH
XPS Intensity (arb. units)
-548
-546
-544
-542
-540
-538
Binding Energy (eV)

(Figure 2)

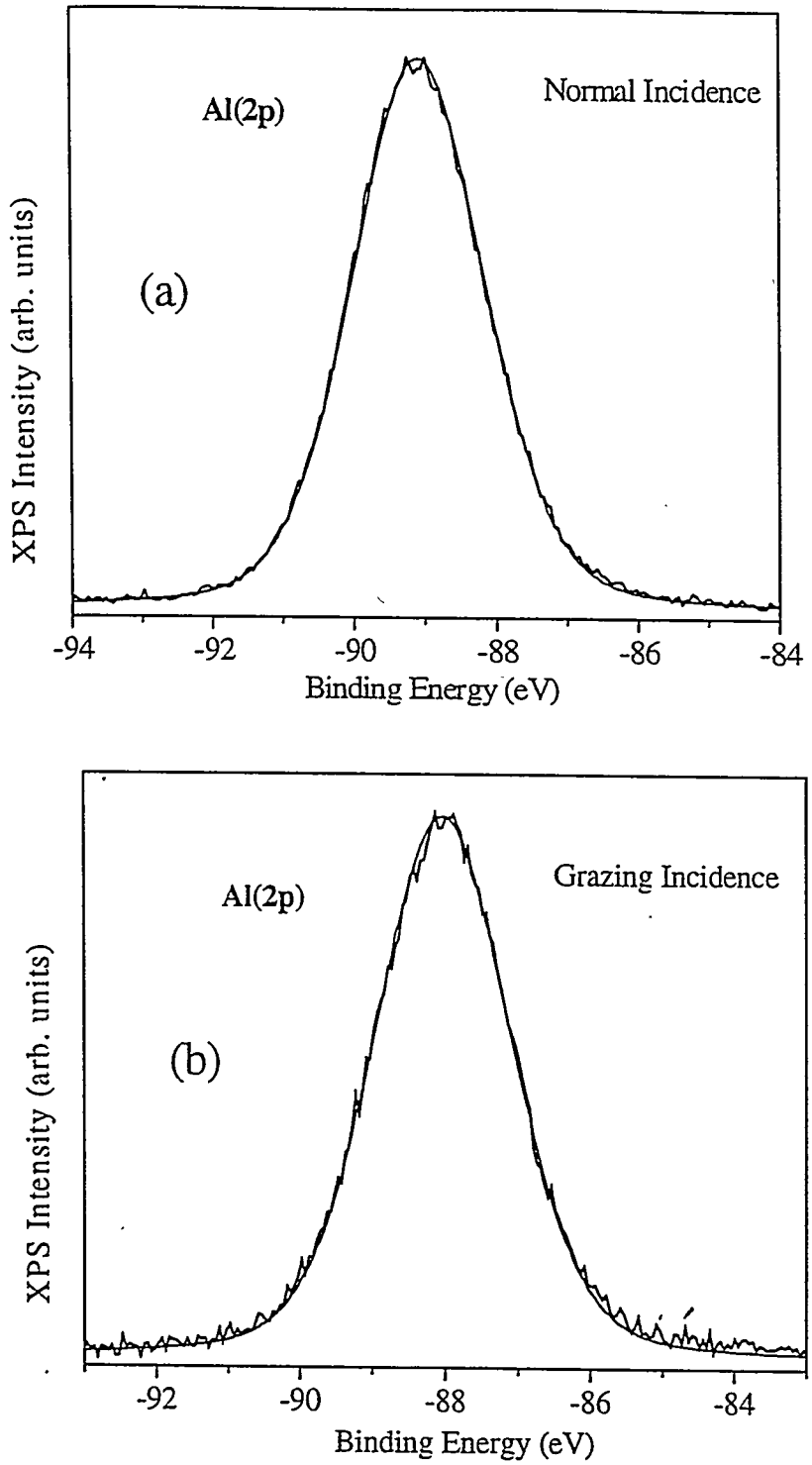
Al(2p)
Normal Incidence
(a)
XPS Intensity (arb. units)
-94
-92
-90
-88
-86
-84
Binding Energy (eV)
Al(2p)
Grazing Incidence
(b)
XPS Intensity (arb. units)
-92
-90
-88
-86
-84
Binding Energy (eV)

Figure 3.

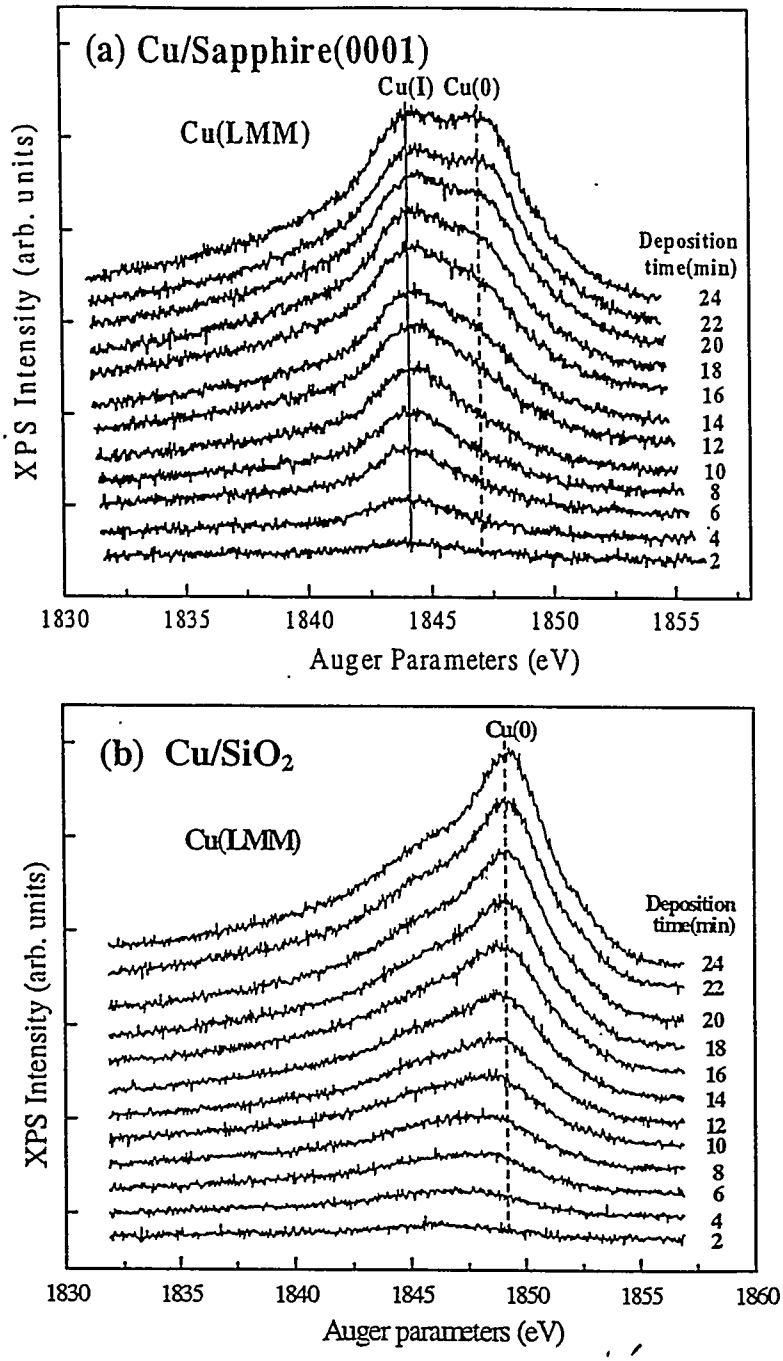
(a) Cu/Sapphire(0001)
Cu(I) Cu(0)
Cu(LMM)
Deposition time(min)
24
22
20
18
16
14
12
10
8
6
4
2
XPS Intensity (arb. units)
1830
1835
1840
1845
1850
1855
Auger Parameters (eV)
(b) Cu/SiO2
Cu(0)
Cu(LMM)
Deposition time(min)
24
22
20
18
16
14
12
10
8
6
4
2
XPS Intensity (arb. units)
1830
1835
1840
1845
1850
1855
1860
Auger parameters (eV)

Figure 4.

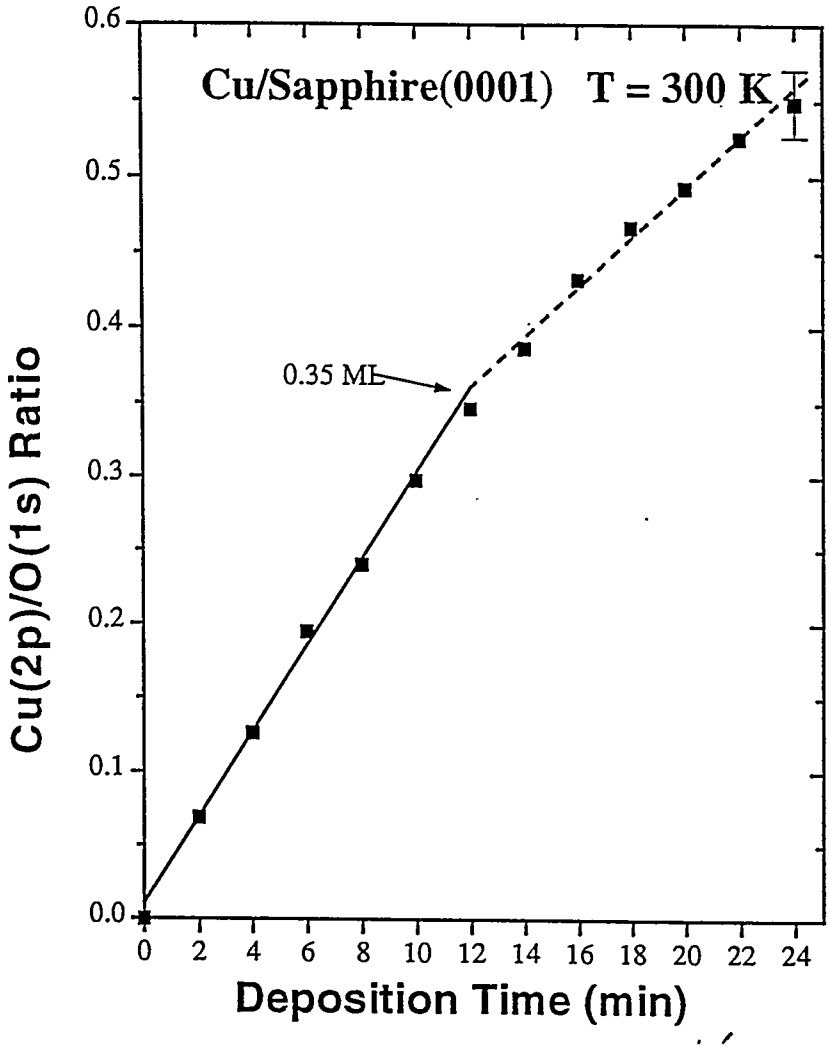
Cu/Sapphire(0001) T = 300 K
0.35 ML
Cu(2p)/O(1s) Ratio
Deposition Time (min)
0.0
0.1
0.2
0.3
0.4
0.5
0.6
0
2
4
6
8
10
12
14
16
18
20
22
24

Figure 5

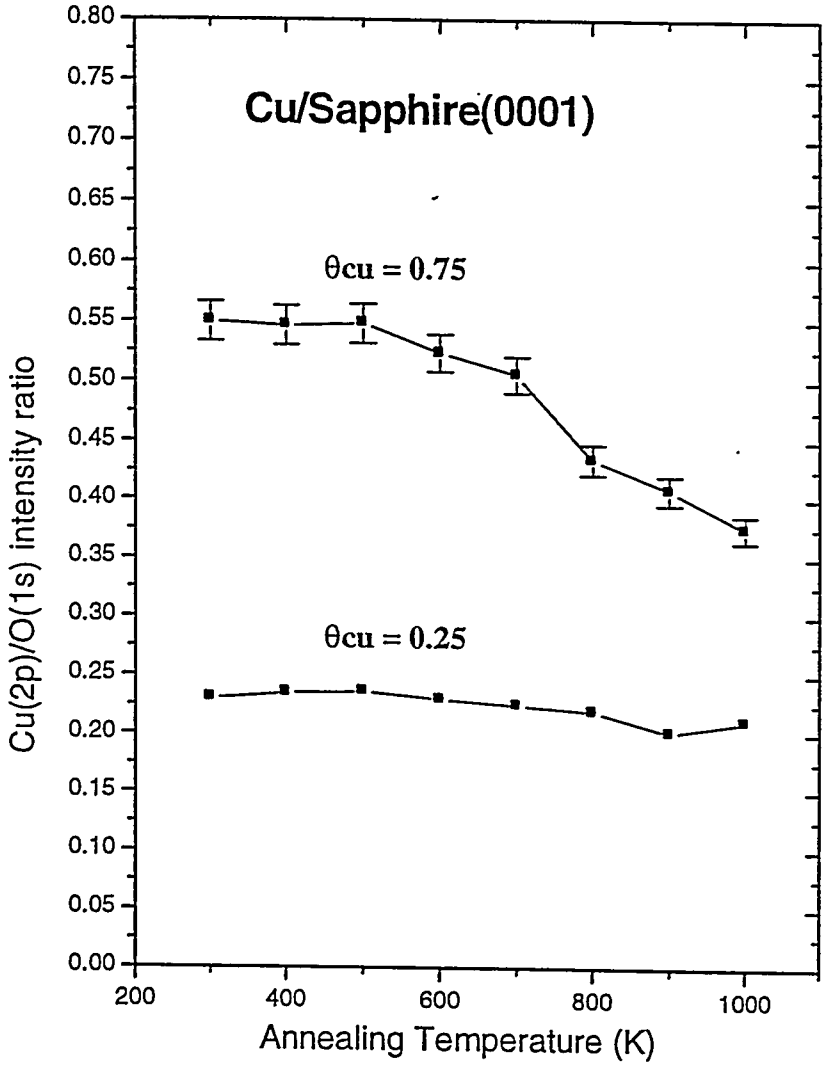
Cu/Sapphire(0001)
θcu = 0.75
θcu = 0.25
Cu(2p)/O(1s) intensity ratio
Annealing Temperature (K)
0.80
0.75
0.70
0.65
0.60
0.55
0.50
0.45
0.40
0.35
0.30
0.25
0.20
0.15
0.10
0.05
0.00
200
400
600
800
1000

Figure 6.

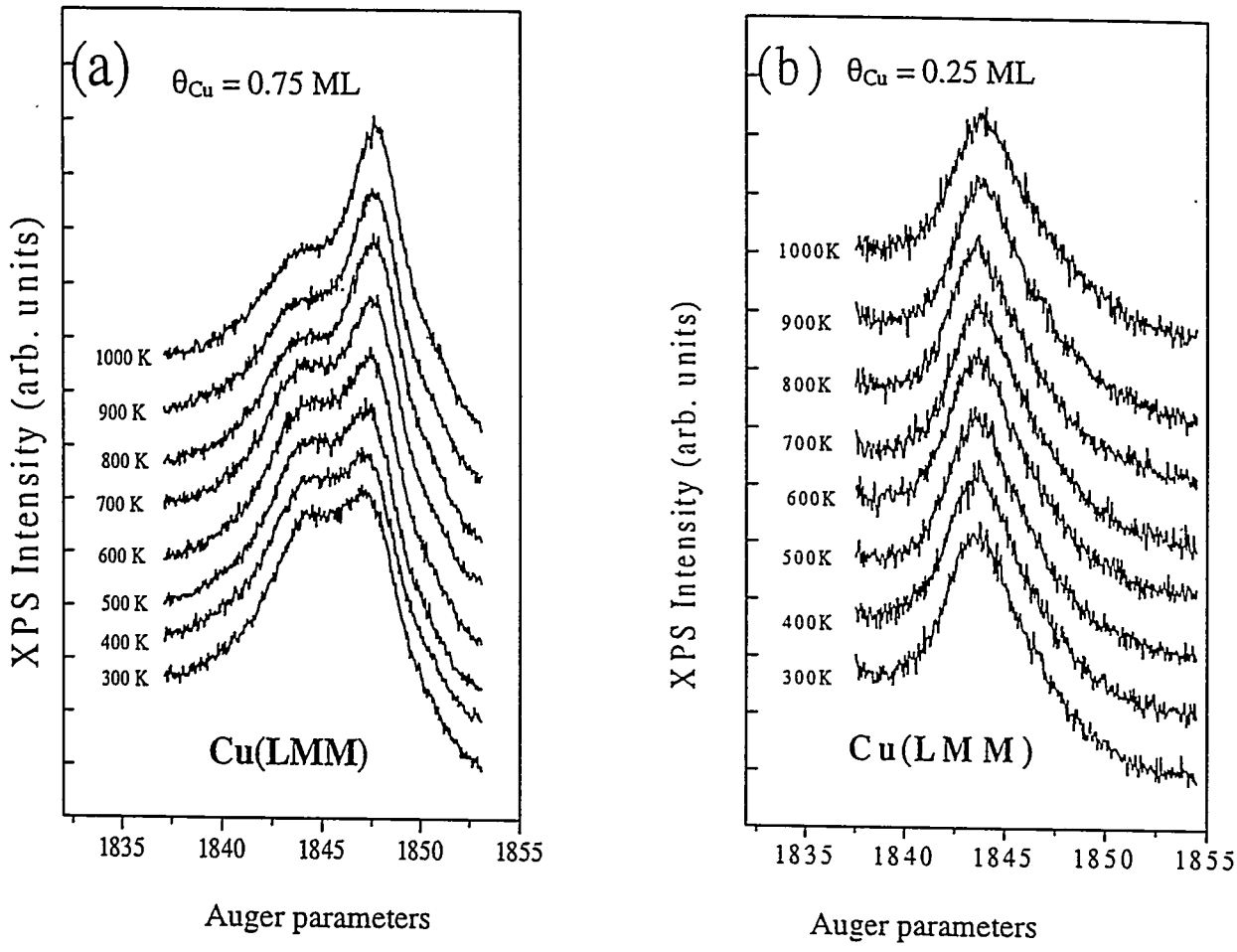
(a)
θCu = 0.75 ML
1000 K
900 K
800 K
700 K
600 K
500 K
400 K
300 K
Cu(LMM)
XPS Intensity (arb. units)
1835
1840
1845
1850
1855
Auger parameters
(b)
θCu = 0.25 ML
1000K
900K
800K
700K
600K
500K
400K
300K
Cu(LMM)
XPS Intensity (arb. units)
1835
1840
1845
1850
1855
Auger parameters

Figure 7.